

Supporting Information for

Phase Regulation and Defect Passivation Enabled by Phosphoryl Chloride Molecules for Efficient Quasi-2D Perovskite Light-Emitting Diodes

Mingliang Li^{1, 2, †}, Yaping Zhao^{2, †}, Jia Guo^{3, *}, Xiangqian Qin², Qin Zhang², Chengbo Tian², Peng Xu², Yuqing Li², Wanja Tian², Xiaoja Zheng¹, Guichuan Xing³, Wen-Hua Zhang^{1, 5, *}, and Zhanhua Wei^{2, 4, *}

¹Sichuan Research Center of New Materials, Institute of Chemical Materials, China Academy of Engineering Physics, Chengdu 610200, P. R. China

²Xiamen Key Laboratory of Optoelectronic Materials and Advanced Manufacturing, Institute of Luminescent Materials and Information Displays, College of Materials Science and Engineering, Huaqiao University, Xiamen 361021, P. R. China

³Joint Key Laboratory of the Ministry of Education, Institute of Applied Physics and Materials Engineering, University of Macau, Taipa, Macau 999078, P. R. China

⁴Innovation Laboratory for Sciences and Technologies of Energy Materials of Fujian Province (IKKEM), Xiamen 361005, P. R. China

⁵School of Materials and Energy, Yunnan University, Kunming 650050, P. R. China

†Mingliang Li and Yaping Zhao contributed equally to this work.

*Corresponding authors. E-mails: jiaguo@um.edu.mo (Jia Guo); wenhuazhang@ynu.edu.cn (Wen-Hua Zhang); weizhanhua@hqu.edu.cn (Zhanhua Wei)

Supplementary Figures and Table

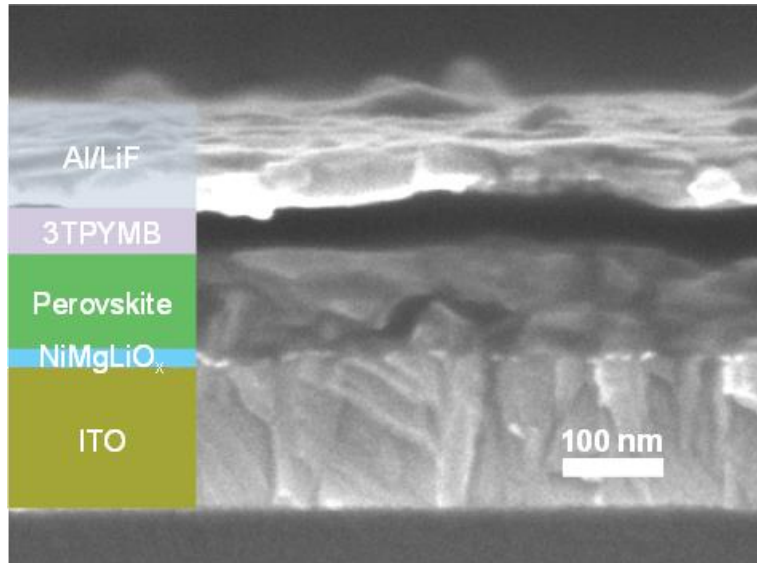


Fig. S1 The cross-sectional SEM image of the Pero-LEDs based on BOPCl-Pero film

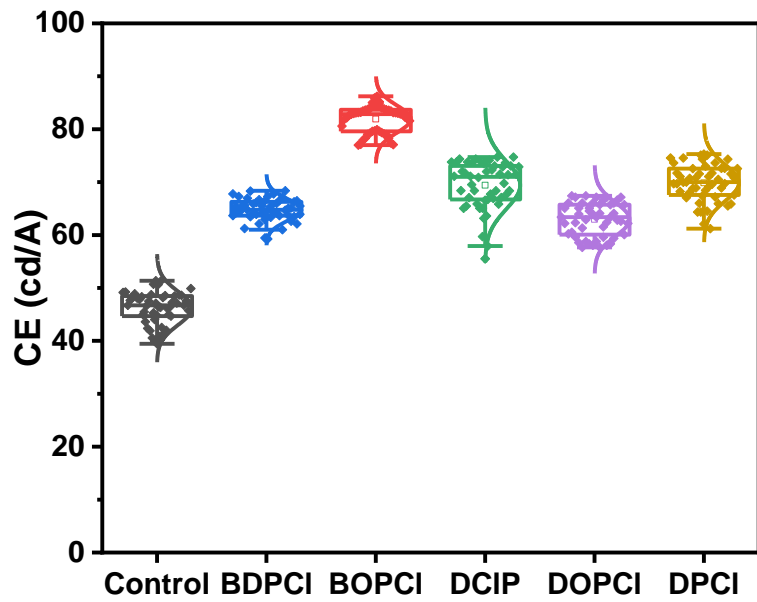


Fig. S2 CE_{max} histogram of the best 50 Pero-LEDs fabricated with Control-Pero films and other perovskite films modified by various phosphoryl chloride molecules

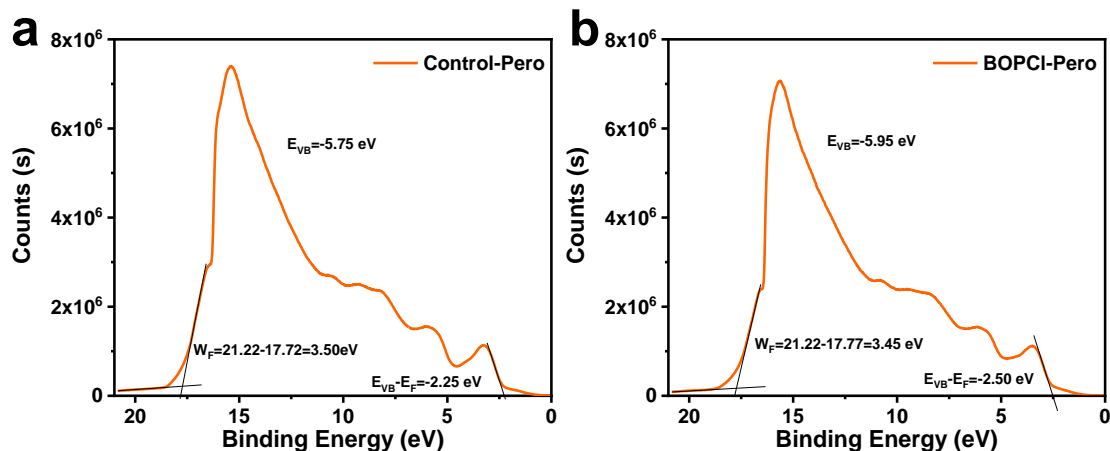


Fig. S3 UPS date of the (a) Control-Pero and (b) BOPCl-Pero films

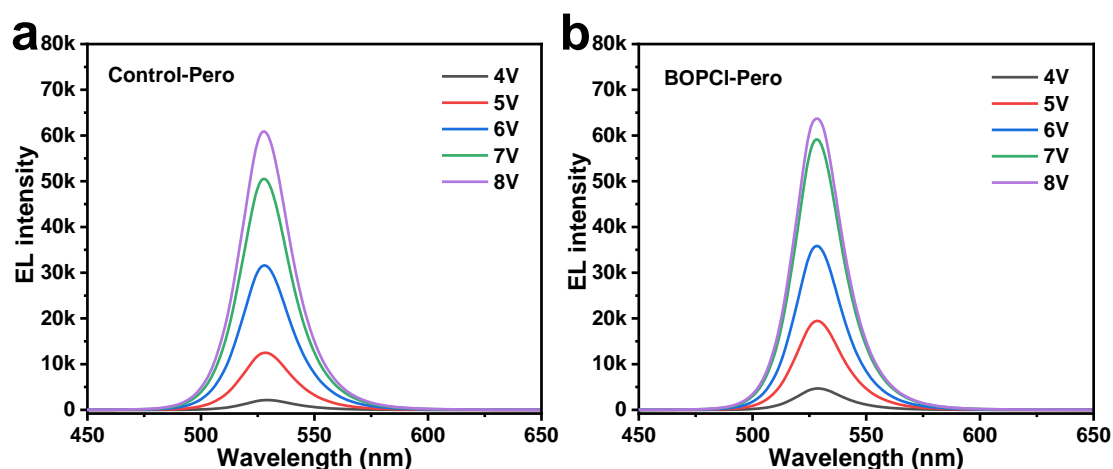


Fig. S4 EL spectra of the Pero-LEDs based on (a) Control-Pero and (b) BOPCl-Pero films

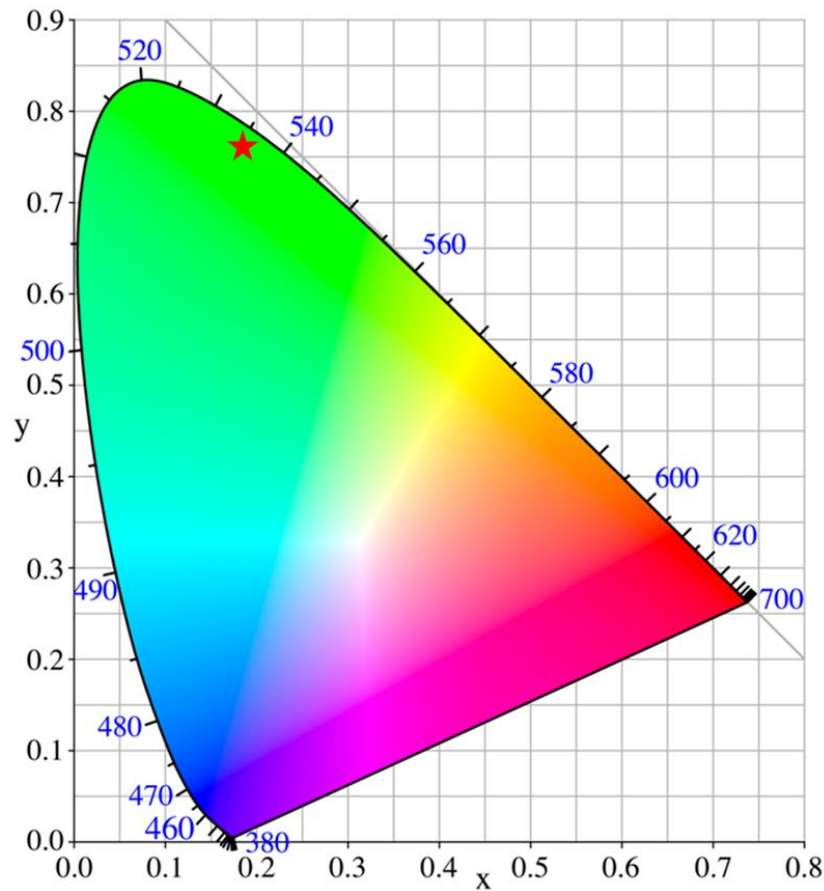


Fig. S5 CIE coordinate of Pero-LEDs based on BOPCl-Pero film

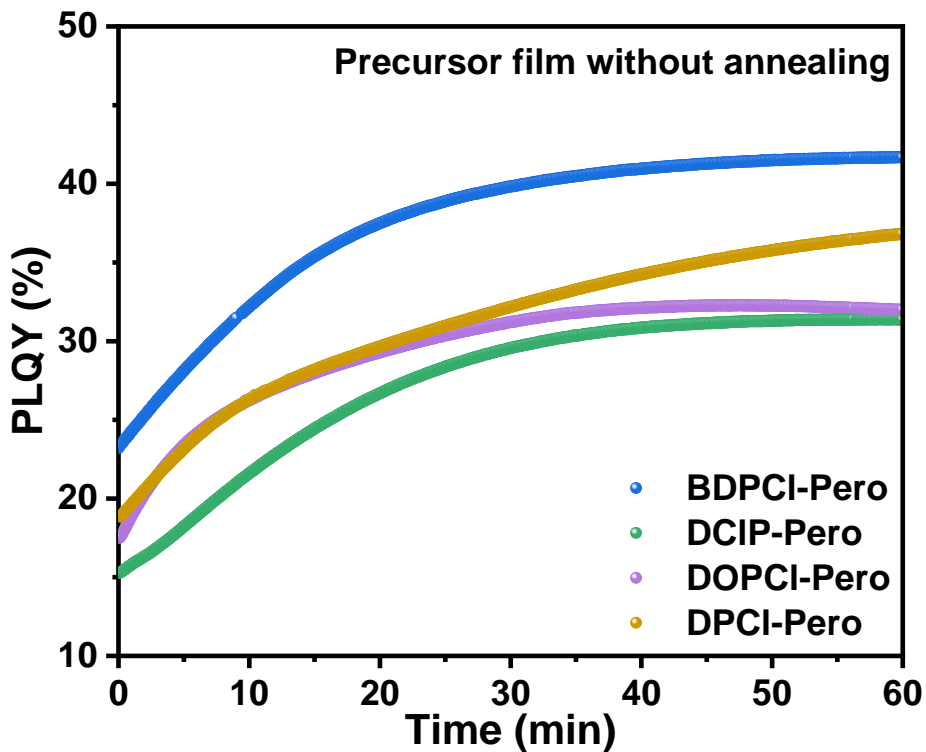


Fig. S6 PLQY evolution of the BDPCI, DCIP, DOPCI and DPCI-Pero precursor films without annealing

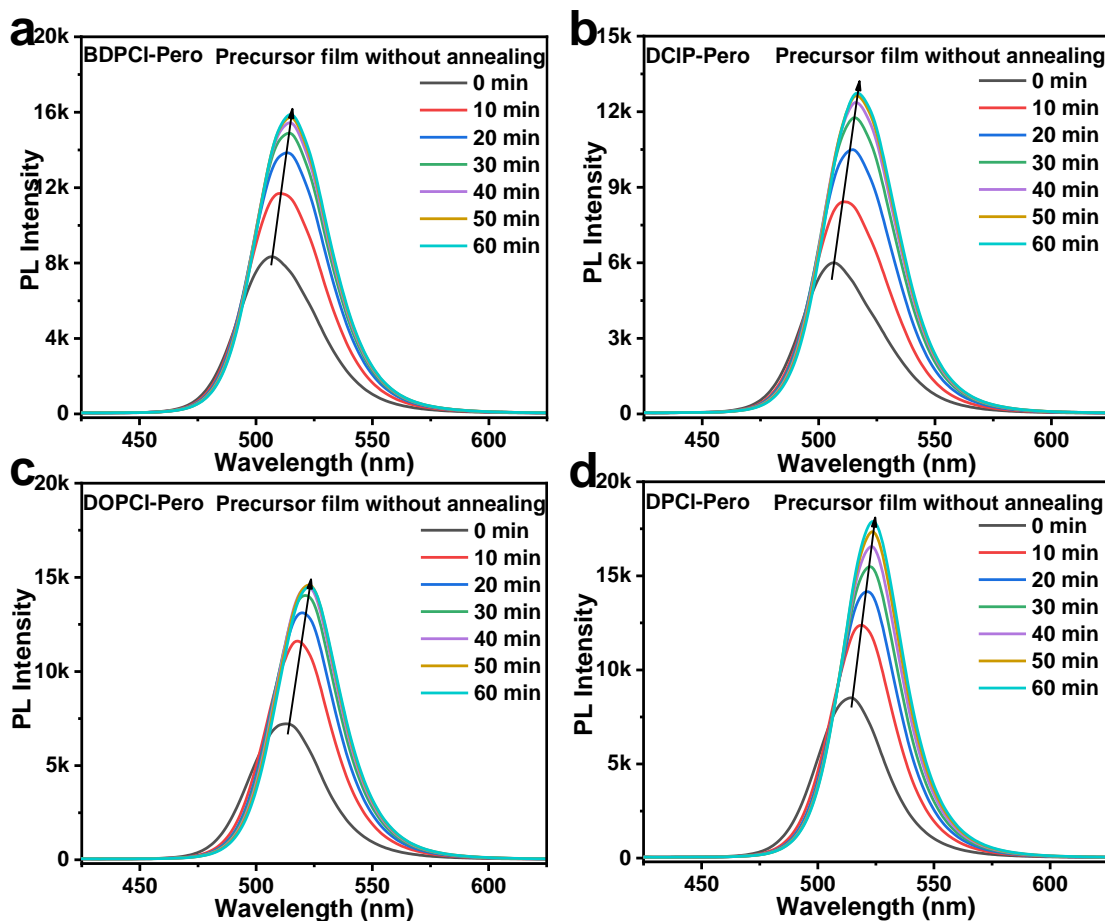


Fig. S7 The corresponding PL spectra for the PLQY evolution of the BDPCI, DCIP, DOPCI and DPCI-Pero precursor films without annealing

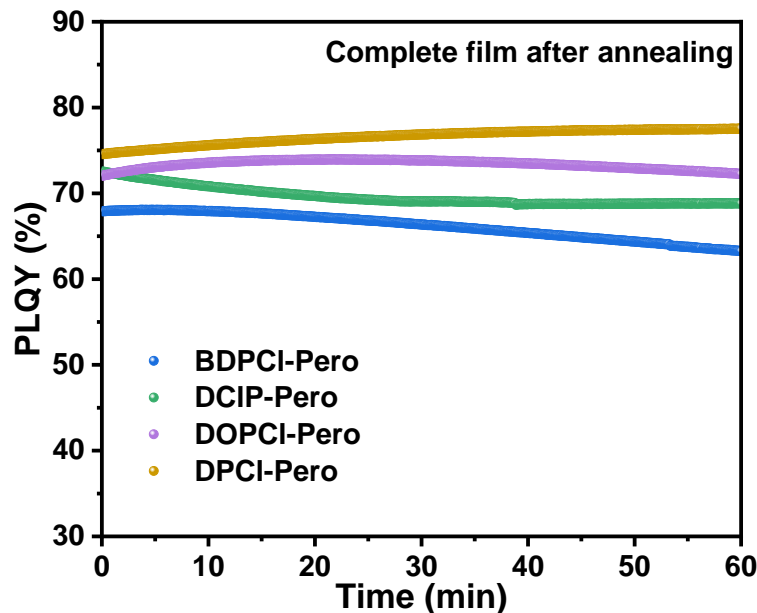


Fig. S8 PLQY evolution of the BDPCI, DCIP, DOPCI and DPCI-Pero complete films after annealing

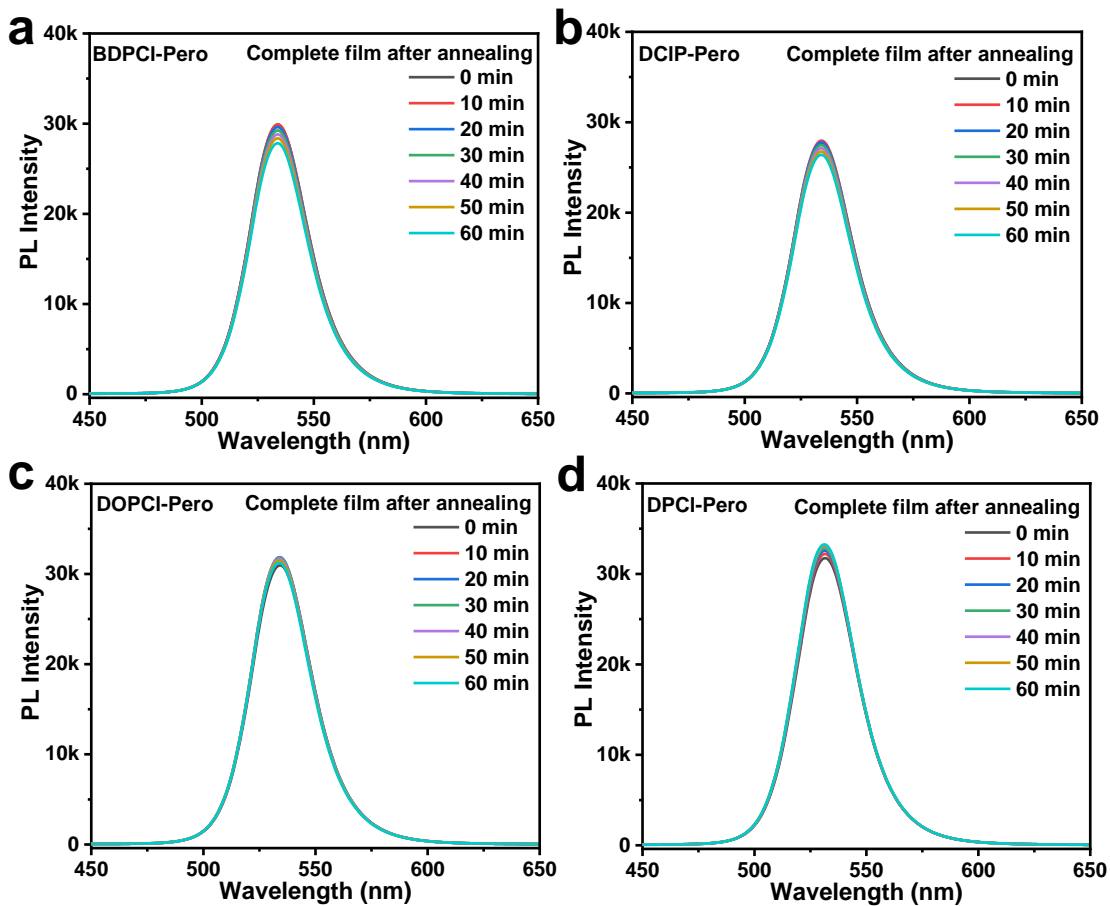


Fig. S9 The corresponding PL spectra for the PLQY evolution of the BDPCI, DCIP, DOPCI and DPCI-Pero complete films after annealing

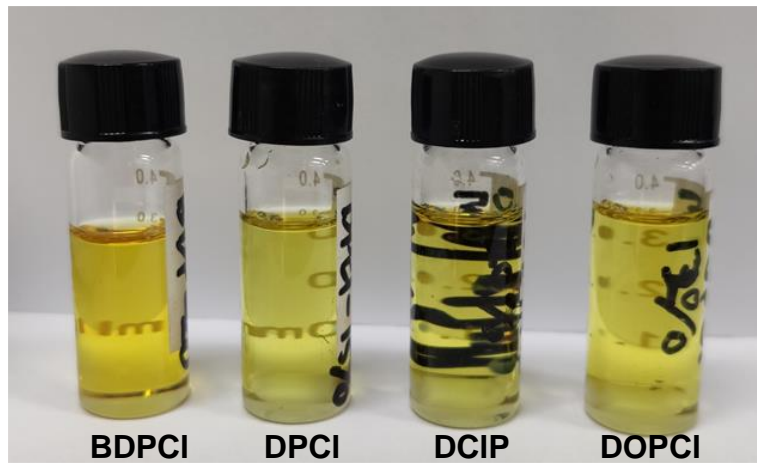


Fig. S10 Photographs of perovskite precursor with BDPCI, DPCI, DCIP and DOPCI

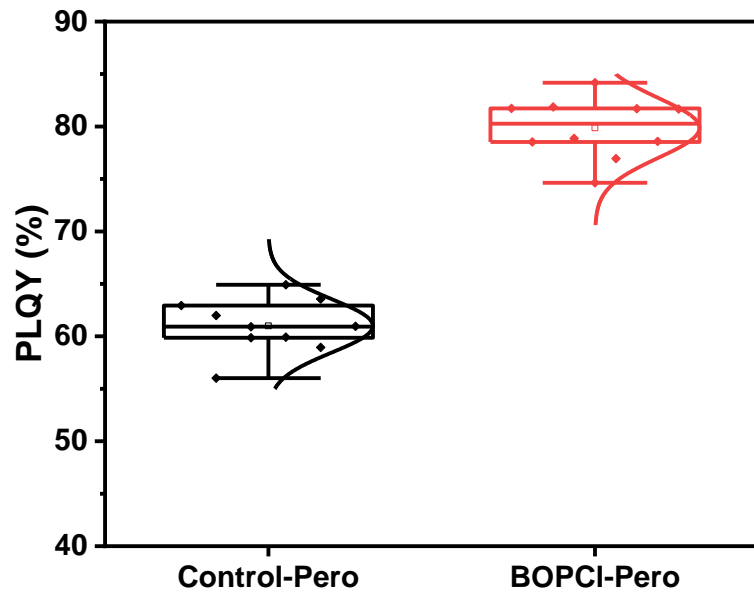


Fig. S11 PLQY histogram of the 10 films of Control-Pero and BOPCl-Pero films

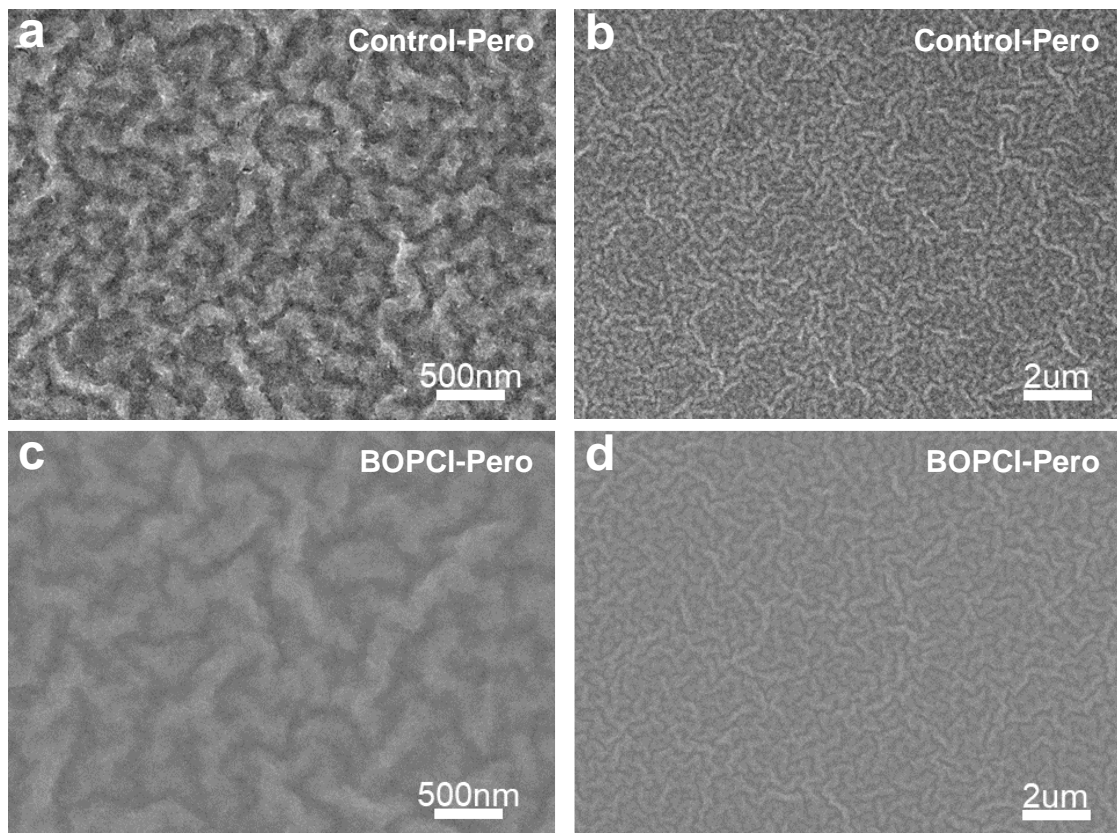


Fig. S12 SEM images of (a, b) Control-Pero and (c, d) BOPCl-Pero films

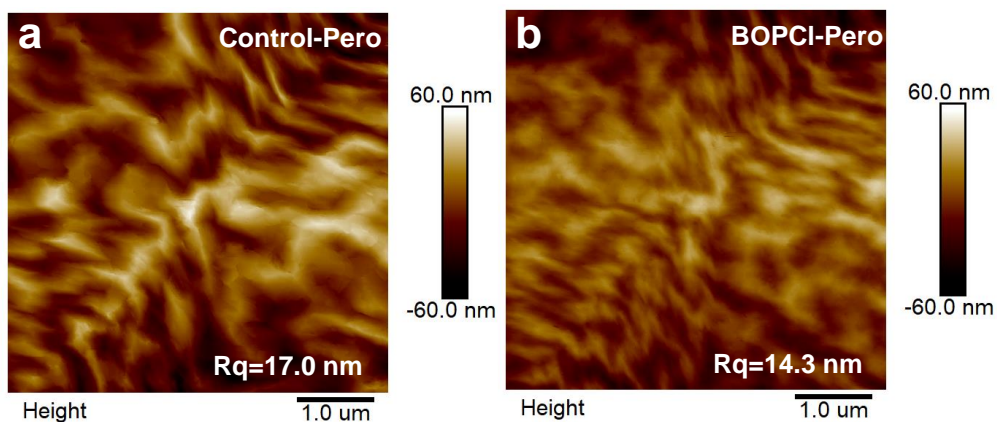


Fig. S13 AFM images of (a) Control-Pero and (b) BOPCl-Pero films

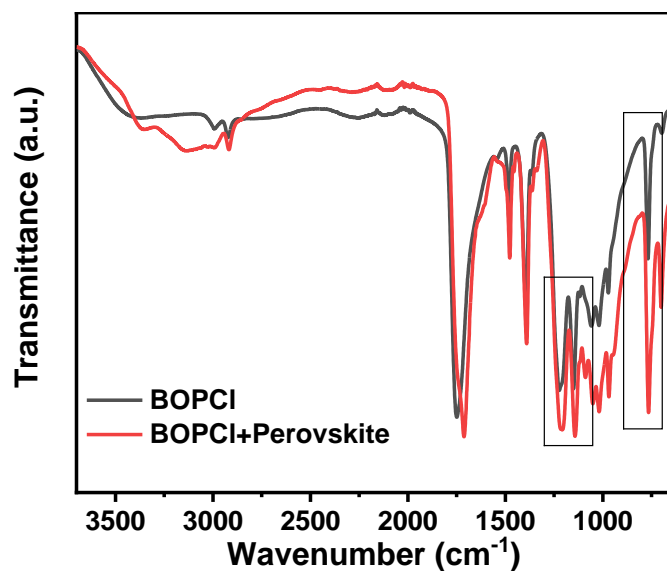


Fig. S14 The full FTIR spectra ranging from 650 to 3700 cm^{-1} of the BOPCl and BOPCl-Pero films

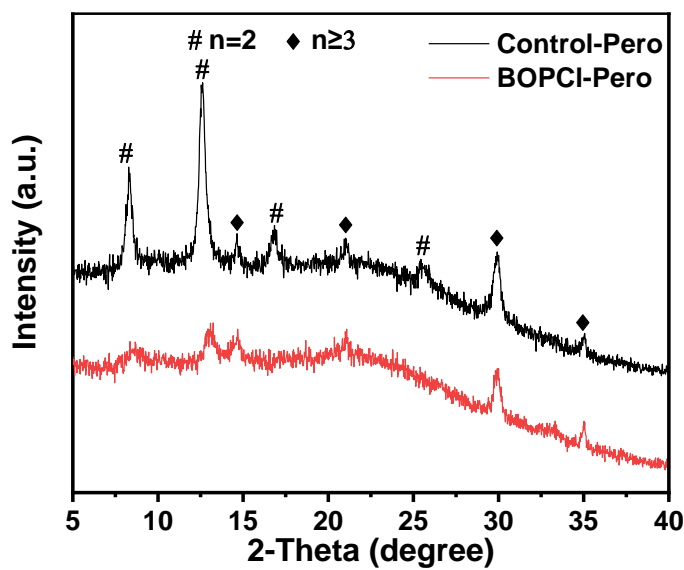


Fig. S15 XRD patterns of the Control-Pero and BOPCl-Pero films

Table S1 Fitting results of the TRPL decay curves of the Control-Pero and BOPCl-Pero films

	τ_1 (ns)	A ₁	τ_2 (ns)	A ₂	τ_3 (ns)	A ₃	χ^2 (%)	τ_{ave} (ns)
Control-Pero	10.17	0.28	1.02	0.66	53.4	0.06	99.9	29.85
BOPCl-Pero	13.47	0.63	41.48	0.35	242.06	0.02	99.9	67.81